Combustion Products of 1,3-Butadiene are Cytotoxic and Genotoxic to Human Bronchial Epithelial Cells

W. James Catallo,[1] Christopher H. Kennedy,[1,2] William Henk,[1] Steven A. Barker,[1] Stephen C. Grace,[3,4] and Arthur Penn[1]

[1]Department of Comparative Biomedical Sciences, School of Veterinary Medicine, Louisiana State University, Baton Rouge, Louisiana, USA; [2]National Cancer Institute, Division of Cancer Prevention, Bethesda, Maryland, USA; [3]Biodynamics Institute, Louisiana State University, Baton Rouge, Louisiana, USA; [4]Department of Biology, University of Arkansas, Little Rock, Arkansas, USA

Adverse health effects of airborne toxicants, especially small respirable particles and their associated adsorbed chemicals, are of growing concern to health professionals, governmental agencies, and the general public. Areas rich in petrochemical processing facilities (e.g., eastern Texas and southern California) chronically have poor air quality. Atmospheric releases of products of incomplete combustion (e.g., soot) from these facilities are not subject to rigorous regulatory enforcement. Although soot can include respirable particles and carcinogens, the toxicologic and epidemiologic consequences of exposure to environmentally relevant complex soots have not been well investigated. Here we continue our physico-chemical analysis of butadiene soot and report effects of exposure to this soot on putative targets, normal human bronchial epithelial (NHBE) cells. We examined organic extracts of butadiene soot by gas chromatography–mass spectrometry (GC–MS), probe distillation MS, and liquid chromatography (LC)–MS–MS. Hundreds of aromatic hydrocarbons and polycyclic aromatic hydrocarbons with molecular mass as high as 1,000 atomic mass units were detected, including known and suspected human carcinogens (e.g., benzo(*a*)pyrene). Butadiene soot particles also had strong, solid-state free-radical character in electron spin resonance analysis. Spin-trapping studies indicated that fresh butadiene soot in a buffered aqueous solution containing dimethylsulfoxide (DMSO) oxidized the DMSO, leading to CH_3• radical formation. Butadiene soot DMSO extract (BSDE)-exposed NHBE cells displayed extranuclear fluorescence within 4 hr of exposure. BSDE was cytotoxic to > 20% of the cells at 72 hr. Morphologic alterations, including cell swelling and membrane blebbing, were apparent within 24 hr of exposure. These alterations are characteristic of oncosis, an ischemia-induced form of cell death. BSDE treatment also produced significant genotoxicity, as indicated by binucleated cell formation. The combination of moderate cytotoxicity and genotoxicity, as occurred here, can be pro-carcinogenic. *Key words*: blebbing, BSDE, butadiene soot, fluorescence, free radicals, human bronchial epithelial cells, PAHs. *Environ Health Perspect* 109:965–971 (2001). [Online 12 September 2001]
http://ehpnet1.niehs.nih.gov/docs/2001/109p965-971catallo/abstract.html

Cardiovascular disease and lung cancer are among the leading causes of death both in Louisiana and throughout the rest of the United States. Age-adjusted death rates are higher in Louisiana than in the rest of the country for both groups of diseases (*1*). Additionally, the death rate from chronic obstructive pulmonary disease is 58% higher in Louisiana than the national average (*2*).

Increasingly, researchers have focused on airborne particles as causes of respiratory (and more recently, in cardiovascular) disease. Adsorbed organic compounds have been implicated in many of the systemic and molecular responses of respiratory system cells exposed to diesel exhaust particles (*3–6*). Studies with residual oil fly ash (ROFA) particles have demonstrated a role for particle-associated metals in inducing inflammatory responses in respiratory cells (*7,8*).

Epidemiologic evidence from the past decade has correlated increased respiratory morbidity and mortality with exposures to small airborne particles. National Ambient Air Quality Standards issued by the U.S. Environmental Protection Agency in 1997 (*9*), shifting the focus from larger particles (≤ 10 μm) to those ≤ 2.5 μm (so called $PM_{2.5}$), reflect this.

Among the most common origins of airborne particles, industrial point sources [i.e., major facilities, each emitting ≥ 10 tons/yr of specific hazardous air pollutants (HAPs) or ≥ 25 tons/yr of a mixture of HAPs] are of particular concern in Louisiana.

In 1997, Louisiana ranked 2nd in the United States in total releases of chemicals on the Toxic Resource Inventory, which is an incomplete survey of the thousands of compounds that can be released into the air. By a wide margin, East Baton Rouge Parish exceeds all other Louisiana parishes—and also ranks in the top 10% of all U.S. counties—in "Person Days in Exceedance of National Ambient Air Quality Standards" (*10*). In Louisiana, the 16 parishes with the highest noncancer cumulative hazard index are all in the southeastern part of the state, where many large petrochemical facilities are located (*11*). Fourteen of the 16 parishes with the highest added cancer risk from hazardous air pollutants also are in this region (*11*).

In the United States, particularly in southern Louisiana and eastern Texas, there is a substantial and growing processing capacity in C_2–C_8 hydrocarbon streams for chemical manufacture [~ 150 billion pounds annually (*12*)]. For economic, regulatory, and technical reasons, flaring of waste or fugitive volatile organic chemicals (VOCs) occurs regularly at many refineries and chemical plants. Light fractions of crude oils are flared routinely, as are purged materials from reforming and cracking plants. VOC releases to the atmosphere are subject to more stringent regulatory reporting than are releases of products of incomplete combustion (PICs, such as soot) including respirable particles and carcinogenic chemicals.

We have been studying combustion product mixtures associated with selected economically and industrially important VOCs (e.g., 1,3-butadiene) and liquid hydrocarbon mixtures [e.g., crude oils, diesel fuel (*12*)]. When 1,3-butadiene and other substrates found in VOC mixtures (e.g., propane, propylene, butane, vinylacetylene) are burned in air, substantial amounts of polynuclear aromatic hydrocarbons (PAHs) and fine particulates (< 2.5 μm) are generated (*12*). Many of the individual chemicals found in VOC combustion mixtures are toxic and mutagenic. Nevertheless, virtually no attention has been paid to the toxicologic and epidemiologic relevance of PICs from VOC burns.

The purpose of this work is to provide additional physico-chemical analysis of combustion residues from 1,3-butadiene (*12*) and describe the pleiotropic responses of putative targets, normal human bronchial epithelial (NHBE) cells, following exposures to these residues. We evaluated these residues to gain insight into the chemical

Address correspondence to A. Penn, Department of Comparative Biomedical Sciences, School of Veterinary Medicine, Louisiana State University, Skip Bertman Drive, Baton Rouge, LA 70803 USA. Telephone: (225) 578-9760. Fax: (225) 578-9769. E-mail: apenn@mail.vetmed.lsu.edu

This work was supported in part by a Grant-in-Aid from the American Heart Association.

Received 18 January 2001; accepted 18 March 2001.

fine structure of the mixture, particularly with respect to PAHs in the semivolatile [78–300 atomic mass units (amu)] and high molecular weight range (300–1,000 amu); the free radicals present in the butadiene soot; and the cytotoxic, genotoxic, and morphologic alterations in NHBE cells following acute exposures to a dimethylsulfoxide (DMSO) extract of this butadiene soot (BSDE). The BSDE was composed of particles of a small (< 0.45 μm), highly respirable size that would be accessible to the NHBE cells *in vivo*.

Materials and Methods

Combustion of 1,3-butadiene and recovery of products of incomplete combustion. Gas-phase 1,3-butadiene (99%; Aldrich, Milwaukee, WI) was introduced at room temperature to a small (20 cm) steel burner at slow feed rates (e.g., 0.5–5 mL/sec). The resulting PICs were trapped on solvent-clean glass fiber filters. These materials were collected and subjected to the treatments and extraction procedures summarized below.

Sample analysis. Weighed soot samples were Soxhlet-extracted for 6 hr using dichloromethane. This extract was dried (Na_2SO_4) and analyzed by gas chromatography-mass spectrometry (GC-MS). We performed semi-quantitation using standard calibration files and/or direct comparisons with internal standards (Ultra Scientific, Kingston, RI). We analyzed heavy fractions using benzene/toluene as the extraction solvents (1:1; v/v).

For electron spin resonance (ESR) studies, we obtained solvent-extractable free radicals from 1,3-butadiene soot from brief liquid–solid extractions with ultra-pure toluene, DMSO:water (4:1, v/v), n-hexane, and 3% aqueous sodium dodecyl sulfate. We membrane-filtered the suspensions (0.45 μm) with glass syringes and Teflon cartridges and centrifuged them at 10,000 rpm for 20 min before analysis.

We prepared BSDE for cell culture studies by dissolving the butadiene soot in DMSO and then membrane-filtered it (0.45 μm) to yield a stock solution (25 mg soot/mL DMSO) that was stored at 4°C.

Mass spectrometry. We examined toluene and DMSO extracts of butadiene soot by probe distillation/electron impact in a single quadrapole mass spectrometer (PDMS; Shimadzu Instruments, Columbia, MD). In the full scan mode, mass range 78–700 amu was scanned. We performed further studies with a Fisons (Beverly, MA) liquid chromatography-tandem mass spectrometer (LC-MS-MS), equipped with microbore LC columns. We conducted analyses using electrospray positive and negative ion modes as well as atmospheric chemical ionization (+/-) modes. We assessed the particles using direct exposure probe MS/MS, analyzing the major peaks from high-temperature (up to 1,200°C) distillation of the particulate residue from a heated filament.

Nitration. We performed nitration experiments with known volumes of liquid NO_2, which was prepared as needed and maintained frozen at –70°C between experiments. The liquid NO_2 was brought to room temperature and the resulting vapors either were equilibrated briefly with combustion residues on filters (postcombustion nitration) or premixed with the butadiene gas feed and combusted as a mixture. In both settings, we calculated NO_2 vapor concentration in the combustion zone to be 100–200 ppm. Selected NO_2 samples were confirmed by single quadrapole mass spectrometry.

Electroanalysis. BSDE was amended with 1mM tetrabutylammonium perchlorate (Sigma, St. Louis, MO), filtered (0.22 μm), and examined for redox activity at C, Au, and Pt working electrodes (1 mm^2) versus Ag/AgCl reference or Pt wire counter electrodes. We performed differential pulse polarography in the physiologic potential range, i.e., +1,100 mV to –1,100 mV versus Ag/AgCl using a Potentiostat (Cypress Systems, St. Louis, MO).

Preparative thin layer chromatography. We applied BSDE to replicate silica gel thin layer chromatography (TLC) plates (Aldrich). The compounds were eluted with hexane mobile phase at room temperature. Fluorescent and colored bands were marked and then collected by scraping. These fractionated samples were used for selected analyses (below).

Electron spin resonance. We examined dry soot and extracts for free radical signals using a Model 109 Electron Paramagnetic Resonance Spectrometer (ESR; Varian Instruments, Palo Alto, CA). We used cylindric sample tubes for solid soot and the hexane and toluene liquid analyses, and quartz flat cells for the other solvents. The conditions employed were microwave frequency, X-band (~ 9.35 GHz); microwave power, 10 mW; receiver gain, 10^2–10^4; modulation amplitude, 1.0 G; field modulation, 100 kHz; time constant, 1 sec; sweep width, 100 G; center field, typically 3,360 G; determined using α,α–diphenyl-β-picryl hydrazil free radical (DPPH) solid or 1mM solution in DMSO; sweep duration, 16 min.

Ascorbate radical ESR intensity. We extracted soot solids (20 mg) in DMSO and clarified them by centrifugation. We mixed aliquots of this extract with 0.5 mM ascorbate in phosphate buffer, pH 7.4, and determined the intensity of the ascorbate radical by its characteristic ESR doublet at g = 2.0058. In measuring the dose dependence of ascorbate free radical formation by BSDE, we quantified the concentration of the ascorbate radical by double integration of the ESR signal. Fremy's salt was used as a concentration standard.

Spin-trapping. We prepared a solution of the spin-trap α-(4-pyridyl-1-oxide)-*N*-tert-butylnitrone [4-POBN; Aldrich (*13*)] in phosphate buffer, pH 7.4, adding 10% DMSO as an oxidizable substrate. Butadiene soot was bubbled into the spin-trap solution immediately after generation under vacuum. The mixture was allowed to separate into an upper phase containing soot solids and an aqueous phase containing trapped radicals. ESR signals were recorded over 24 hr.

Cell culture. NHBE cells from never-smokers (Strains #2129 & 2505) and bronchial epithelial cell growth medium (BEGM) were purchased from Clonetics (San Diego, CA). The cryopreserved cells (passage 1) were plated on Corning 60 mm plastic tissue culture dishes (Fisher Scientific, Springfield, NJ) precoated with FNC Coating Mix (BRFF, Ijamsville, MD), expanded to about 90% confluence and subcultured.

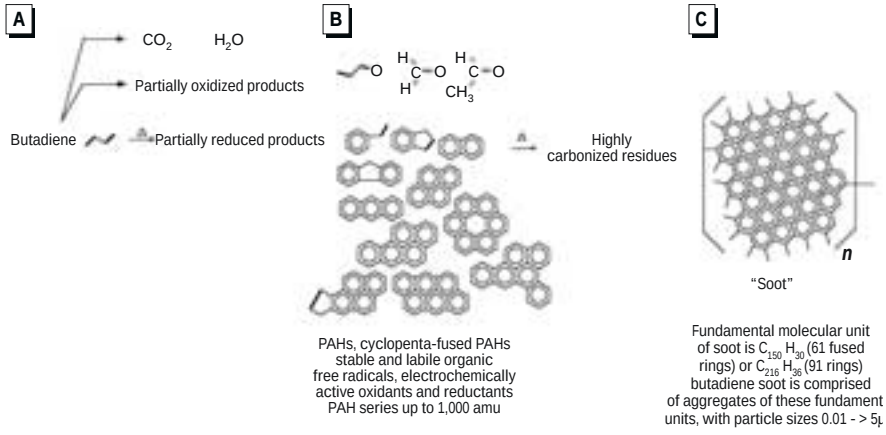

Figure 1. Schematic representation of combustion of 1,3-butadiene showing the genesis of oxidized (*A*,*B*) and reduced products (*C*).

Exposure of NHBE cells to BSDE. NHBE cells (passage 3 or 4) were cultured and expanded to approximately 50% confluence. We added BSDE to fresh BEGM just before exposure. For each treatment group, we prepared dosing solutions by adding BSDE from the stock solution to the total volume of medium (1:100) for the whole group, mixing, and then adding 5 mL of dosing solution to each dish of cells. The treatment groups were vehicle control, 0.1%–1.0% DMSO added to the media; low-dose, 1 µL BSDE (stock = 2.5 mg soot/mL DMSO) added/mL of media; high-dose, 1 µL BSDE (stock = 25 mg soot/mL DMSO) added/mL of media. After treatment, the cells were incubated for 72 hr at 35.5°C in an atmosphere of 95% air/5% CO_2.

Intracellular fluorescence. At periods ranging from 4 to 72 hr after exposure, BSDE- and vehicle control-exposed NHBE cells were viewed at 200× with an inverted phase-contrast fluorescent microscope (Nikon, Garden City, NY) and photographed immediately. Excitation and emission wavelengths were 365 nm and > 420 nm, respectively.

Cytotoxicity. At 72 hr, we stained cells with 0.4% Trypan Blue solution (Sigma) and then fixed them in 2% formaldehyde (pH 7.4). Three fields of 500 cells/dish were scored at 600× to determine the number of white (viable) and blue (nonviable) cells.

Binucleated cells (BNCs). After 72 hr, we washed the cells twice with HEPES-buffered saline, fixed them in 2% formaldehyde (pH 7.4), treated them with 10 µg ribonuclease A (Sigma) (30 min, 37°C), and then stained them with 5 µg propidium iodide (Sigma) overnight at 4°C. Three fields of 500 cells per dish were scored at 600× to determine the number of binucleated cells (*14*). We considered cell cultures to have significantly elevated levels ($p < 0.05$) of BNCs if the number of BNCs per 500 cells was greater than the mean number of BNCs per 500 cells + 2 standard deviations (SDs) for the vehicle control group.

Statistical analysis. For both the cytotoxicity and BNC assays, we compared means of control and BSDE-exposed groups by analysis of variance (ANOVA). We compared differences between group means by the student Newman-Keuls test (alpha = 0.05).

Transmission electron microscopy. We fixed NHBE cell monolayers *in situ* with a mixture of 1.25% glutaraldehyde and 2% formaldehyde in 0.1 M sodium cacodylate for 1 hr at room temperature. We washed the cells in several changes of 0.1M sodium cacodylate containing 5% sucrose; postfixation occurred in 1% OsO_4 in distilled water for 1 hr. Following postfixation, cell monolayers were dehydrated through a graded ethanol series and embedded *in situ* with Epon-Araldite (Electron Microscopy Sciences, Fort Washington, PA). After polymerization, portions of the embedded monolayer were excised and sectioned. We stained the resulting sections with uranyl acetate and lead citrate and examined them with a Zeiss EM-10C transmission electron microscope (Zeiss, Oberkochen, Germany).

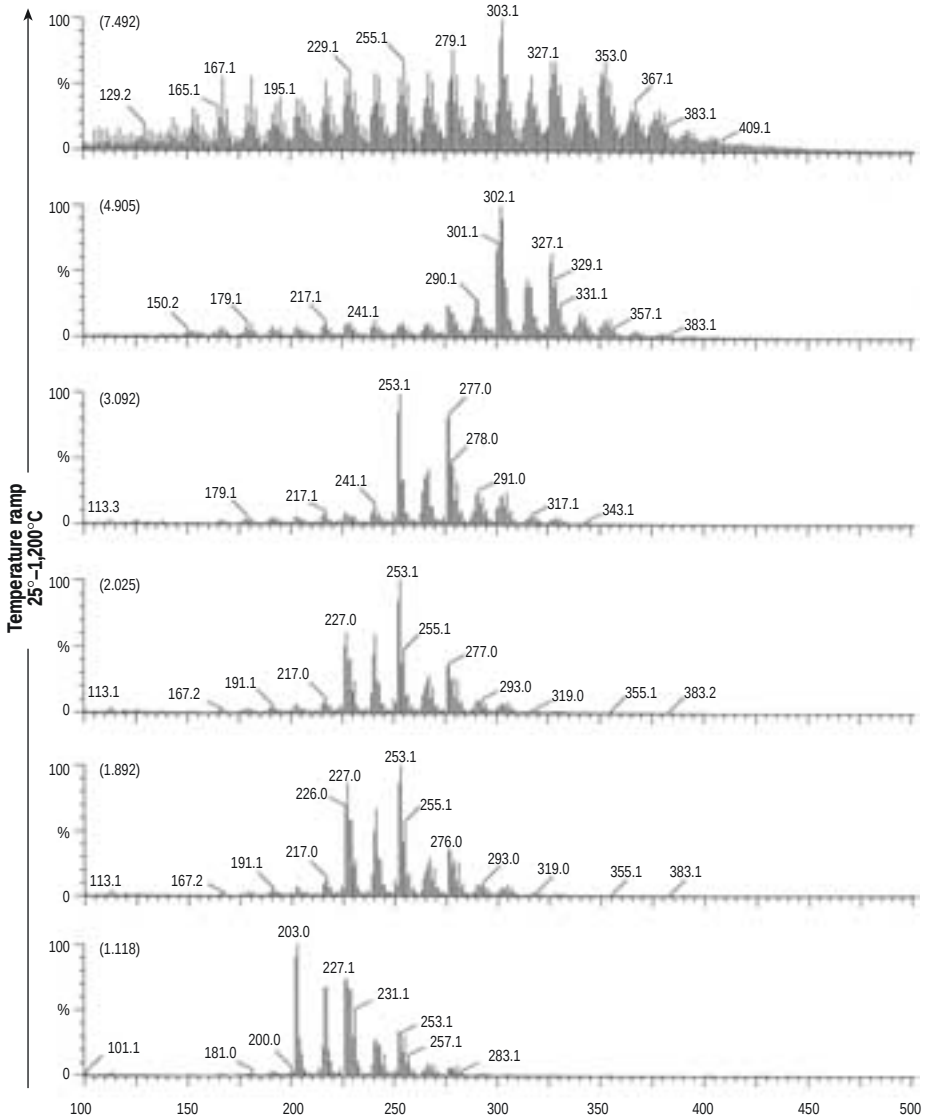

Figure 2. Probe distillation mass spectra of 1,3-butadiene soot in the mass range 100-500 amu (abscissa). A benzene:toluene (1:1) extract of 1,3-butadiene soot was analyzed via positive ion methane chemical ionization on a Fisons Quattro II MS-MS. Each successive scan (bottom → top) represents increasing time (min) after temperature initiation. Relative intensity is normalized for each scan. Nominal resolution = 0.1 amu; positive ion mode chemical ionization (methane).

Results

Combustion of 1,3-butadiene and recovery of products of incomplete combustion. The 1,3-butadiene vapor fire used for generating BSDE had large thermal gradients with temperatures measured *in situ* ranging from 430°C at the edges of the flame to 1,100°C at the cone (*12*). Soot yields varied with fuel flow rate and ranged from 0.1–1.0%, but were constant within the specified flow regime (see "Materials and Methods"). This soot contains a broad and unique range of aromatic hydrocarbons (AHs) and PAHs. In the semivolatile range, the mixture contained hundreds of AHs and PAHs ranging from benzene to coronene. Cyclopenta-fused PAHs also were well represented. Among these compounds were numerous known and suspected human carcinogens, e.g., benzo(*a*)pyrene [B(*a*)P] (Figure 1). We detected PAHs with higher molecular mass, ranging as high as 1,000 amu (not shown), with compounds in the range 228–366 amu well represented (Figure 2; $M+H^{\bullet+}$ masses > 500 not shown) and in large amounts [1,000–5,000 cigarette equivalents of benzofluoranthenes + benzopyrenes + perylene

per gram substrate burned; *m/z* 252; $M+H^{\bullet+}$ masses (i.e., 253.1) shown]. At least four dibenzopyrene isomers [$C_{24}H_{14}$; *m/z* 302; $M+H^{\bullet+}$ masses (i.e., 303.1) shown] also were tentatively identified. Dibenzopyrene isomers are of particular interest because they are found in urban air and most are mutagenic (*15*).

The presence of NO_2 vapors either in the flame or in contact with combustion products produced assemblages of nitrated compounds including nitro- and polynitrotoluenes, -C2-benzenes, -phenols, and PAHs, e.g., -naphthalenes and -fluorene (data not presented). Cocombustion of mixtures of 1,3-butadiene/NO_2 produced more nitration of selected chemicals than did postcombustion NO_2 exposure, but cocombustion also provided much less soot yield than the latter (data not shown).

Electrochemistry. Electrochemical measurements indicated that BSDE was redox active at solid electrodes within an approximate physiologic potential range. Differential pulse polarography showed at least two reduction systems in the positive potential range (+600; +1,100 mV) plus another at –750 mV (Figure 3). These data indicated that butadiene soot constituents may be expected to undergo redox reactions in solution or at adsorption sites in exposed cells. Additional findings showed that these redox systems were not classically reversible (data not presented).

Electron spin resonance (ESR). Soot particles from combustion of pure 1,3-butadiene also had strong solid-state free-radical character in ESR analysis [*g* factor = 2.0028; ~4% spin/weight vs. weak pitch and DPPH standards (Figure 4A)]. Based on the weak pitch standard, the soot contained 1,018 spins/g, comparable to the values for cigarette tar. The radicals present in soot powder were stable for more than one year and could be extracted in organic solvents, although in relatively low yields. The lack of discernible hyperfine structure suggested the presence of a mixture of radical species with overlapping ESR spectra. Alternatively, this could indicate the presence of a solid-state radical. Analyses of fractions from preparative TLC of BSDE showed free radicals only in the soot band, i.e., in the immobile, high molecular weight fraction. Further, filtered, clarified DMSO extracts had less of this radical activity than the dry soot, apparently because only very fine particles remained in these extracts (i.e., the radical was not classically extractable in DMSO).

As a result of these electrochemical and ESR findings, we investigated the effects of several dissolved redox systems on the stable butadiene soot radical signal. Reducing agents including ascorbic acid, glutathione, sodium dithionite, chlorogenic acid, and NADPH had no effect on the intensity or line shape of the soot radical ESR signal (data not presented). Although ascorbic acid was unable to quench the soot radical signal, BSDE did effect the one electron oxidation of ascorbic acid to the semidehydro-ascorbate free radical (Figure 4B). The signal was quasi-stable, suggesting that a redox cycle maintains a steady-state concentration of the ascorbate radical (Figure 4C).

Spin trapping. We examined the oxidizing properties of butadiene soot further using the spin trap, 4-POBN. A 15-line ESR spectrum (Figure 5) arose from two radical

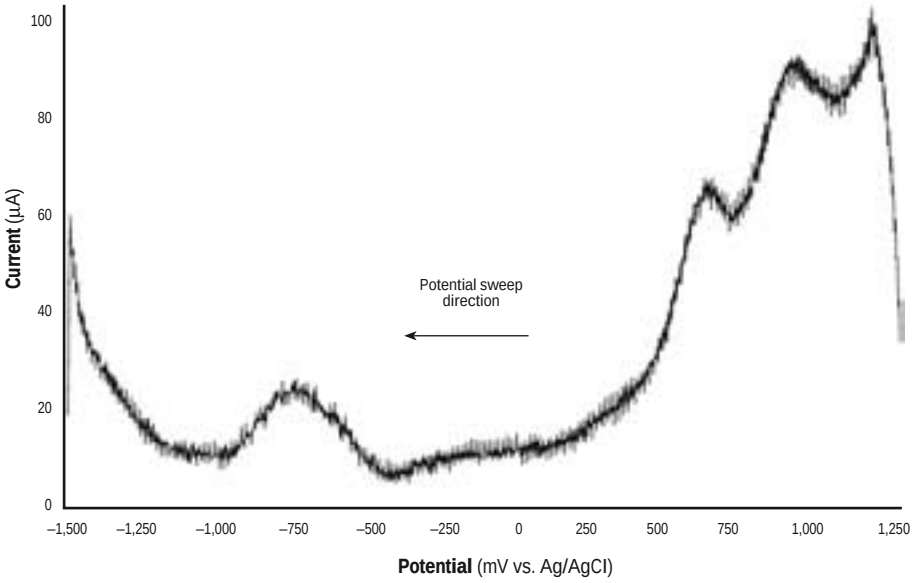

Figure 3. Differential pulse polarogram cathodic sweep, 50 mV/sec. Electroanalysis of 20 mg BSDE in 20 mL buffered protic solvent, dimethylsulfoxide:phosphate-buffered saline, pH 7.4, 1:1 (DMSO:PBS), in a physiologic potential range. Reference control solutions without soot showed no currents in this potential range.

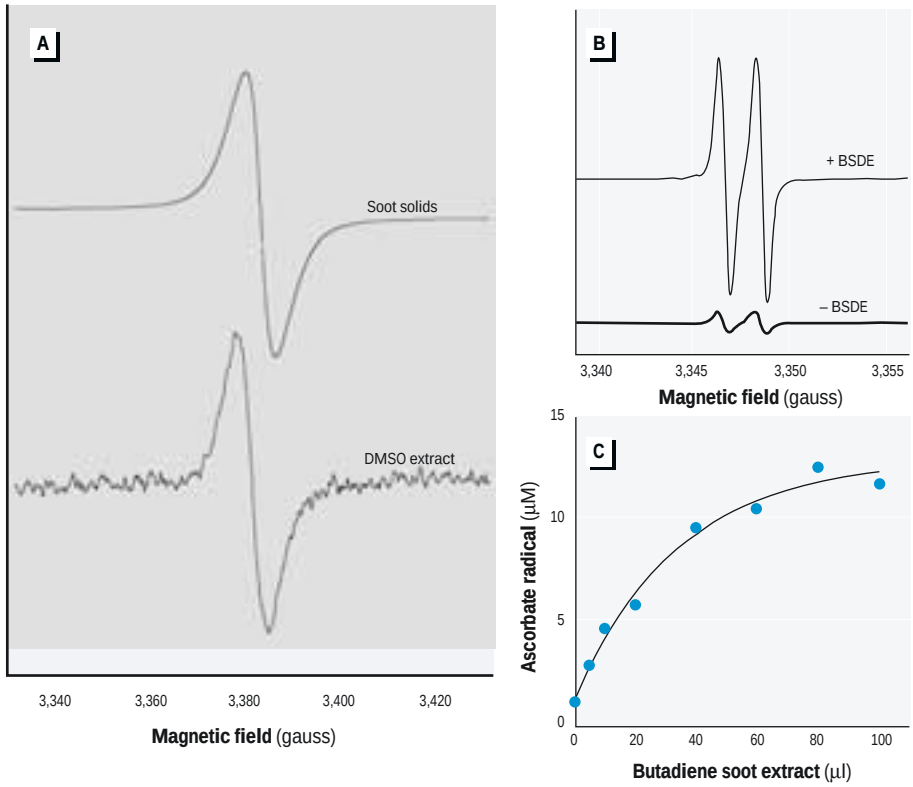

Figure 4. ESR spectra (for measured *g* values, see text). (*A*) Spectra of the stable soot radical solid, and the same signal at 100-fold higher gain in clarified, filtered DMSO extracts. (*B*) The semidehydroascorbyl free radical signal in the presence (top) and absence (bottom) of BSDE. (*C*) Titration curve showing dose-dependent generation of the ascorbyl radical by BSDE.

species, the methyl (CH_3•) adduct of 4-POBN (hyperfine splittings: aN = 16.0 G and aH = 2.8 G) and the hydrogen atom adduct of 4-POBN [aN = 15.8 G and aH (2H) = 10.2 G]. The CH_3• adduct signal intensity increased steadily over the course of the experiment (Figure 5), indicating that the DMSO was being oxidized continuously to form the CH_3• radical, which is trapped by 4-POBN in the aqueous phase.

Intracellular fluorescence in BSDE-exposed NHBE cells. Within 4 hr after exposure to BSDE, extranuclear cell fluorescence was apparent. The fluorescence intensified up to 24 hr, and still was prominent at 72 hr. The increase in intracellular fluorescence was dose-related in BSDE-exposed cells (Figure 6B,D,F). About 30% of NHBE cells in the high-dose group were fluorescent.

BSDE cytotoxicity. We measured Trypan Blue exclusion in NHBE cells 72 hr after a single exposure to BSDE (Table 1). BSDE treatment elicited significant increases in cytotoxicity relative to vehicle controls (ANOVA, F = 54.04). Both low dose (2.5 µg soot/mL) and high dose (25.0 µg soot/mL) BSDE-treated cells exhibited increased cytotoxicity compared with vehicle control cells. In addition, there was significantly greater cytotoxicity in high-dose than in low-dose BSDE-treated NHBE cells (Student Newman-Keuls test, alpha = 0.05).

Induction of BNCs. Unexposed controls, vehicle controls, and NHBE cells exposed to BSDE for 72 hr were stained with propidium iodide and assayed for the presence of BNCs (Table 2). The background level was 18 ± 1 BNCs/500 cells (mean ± SD, n =3) in unexposed controls, so the significance level (mean + 2 SDs, $p < 0.05$) was established as > 20 BNCs/500 cells. There were 20 BNCs/500 cells in the vehicle control group. The ANOVA (F = 52.17) revealed differences between the group means. The high-dose NHBE group had significantly more BNCs than either the low-dose or vehicle-treated groups. There were no differences between the vehicle-control and low-dose groups (Student Newman-Keuls test, alpha = 0.05).

Morphologic alterations. The cytotoxicity measured at 72 hr was preceded by pronounced morphologic changes. These alterations, detected by light microscopy as early as 24 hr after exposure, included cell swelling and rounding as well as apparent plasma membrane irregularities. These changes were examined further by transmission electron microscopy. At 72 hr, DMSO-treated cells displayed normal-sized nuclei with nucleoli, a number of small, mostly perinuclear vacuoles, prominent endoplasmic reticulum (ER), and numerous surface microvilli-like projections (Figure 7A). In contrast, high-dose BSDE-exposed NHBE cells were rounded, with swollen nuclei, no visible nucleoli, vesiculated cytoplasm with large, peripheral cytoplasmic vacuoles, swollen ER cisternae, and loss of surface microvilli-like projections (Figure 7B). The membrane irregularities seen by light microscopy were revealed as numerous rounded surface blebs, some of which had budded off from and were located adjacent to the plasma membrane (Figure 7B). These blebs enclosed amorphous cytoplasmic material.

Discussion

The increased interest in the roles of $PM_{2.5}$ in respiratory and cardiovascular morbidity and mortality has been accompanied by efforts to develop model systems for studying *in vivo* and *in vitro* responses to airborne particulates. ROFA studies have provided data on inflammatory responses of airway epithelial cells to particles containing primarily trace metals (*7,8*). The National Institute

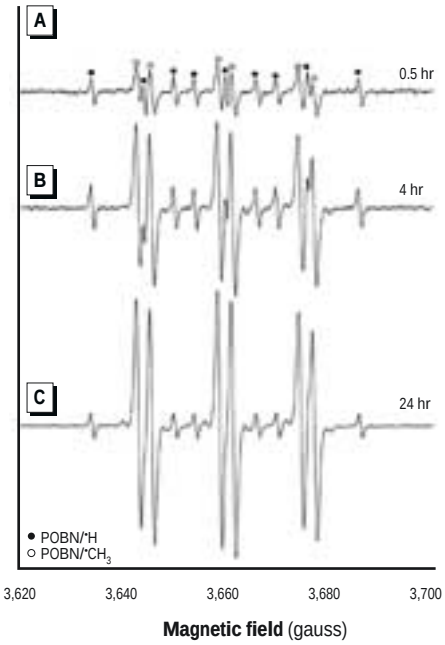

Figure 5. α-(4-pyridyl-1-oxide)-*N*-*tert*-butylnitrone (4-POBN) spin trap results showing time-dependent evolution of •CH_3 radical adducts resulting from oxidation of DMSO by freshly generated butadiene soot particles. The steady-state levels of •H adducts also shown result from POBN chemical reactions *in situ*.

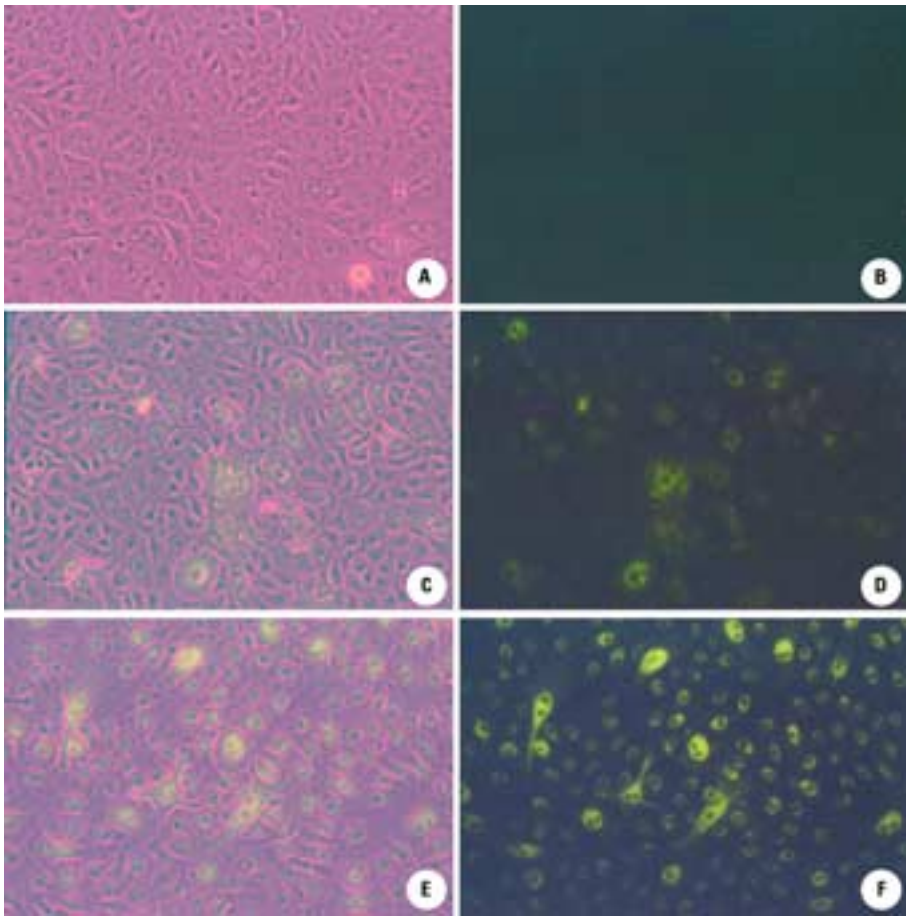

Figure 6. Extranuclear cellular fluorescence in cultured NHBE cells after a single acute exposure to BSDE. Cells were photographed under phase contrast and fluorescence (*A*,*C*,*E*) or under fluorescence only (*B*,*D*,*F*). Vehicle control (*A*,*B*); low dose BSDE (*C*,*D*); high dose BSDE (*E*,*F*). Excitation wavelength = 365 nm, emission wavelength > 420 nm. Magnification = 200×.

of Standards and Technology (Gaithersburg, MD) urban dust mixture (*16*) is a good model for particulates containing low levels of adsorbed organic compounds. On the other hand, pyrogenic yields of hydrocarbons and their product distribution differ dramatically among combustion sources as well as regionally. Thus, additional models of urban/industrial PM mixtures reflecting these differences would be valuable. This is particularly true of pollutant-enriched particulate mixtures that could represent worst cases or upper limits of potential exposure, as well as provide novel toxicologic insights.

The butadiene soot described here is a model for a "real-world" flame product. In the real world, the combustion substrate for uncontrolled burns of low molecular weight petrochemicals generally is a mix of industrial grade C_2–C_8 hydrocarbons, primarily, but not exclusively, 1,3-butadiene. Thus, the levels we describe here of PAHs generated from open flaming of a single pure (> 99%) chemical, 1,3-butadiene, represent a pollutant-enriched situation. The range of products generated from combustion of pure 1,3-butadiene likely is narrower than that produced by combustion of a mix of C_2–C_8 hydrocarbons.

Here we continue the physico-chemical characterization of butadiene soot (*12*) and report our initial observations on the effects of BSDE, a DMSO extract of this soot, on putative targets—NHBE cells.

The combustion product analyses revealed that butadiene soot contains a broad and concentrated range of PAHs and high molecular weight species, including reactive cyclopenta and methylene-bridged species and a series of known and suspected mutagens/carcinogens. The wide range of products found in BSDE, including AHs, PAHs, and free radicals, combined with the small size of the generated particles, indicates that inhalation of BSDE could have deleterious health consequences.

The data presented here were derived from one stock preparation of BSDE. In experiments not reported here, with other stocks prepared under identical burn conditions, no differences were found in either the range or yield of PAHs, as analyzed in two different laboratories by GC/MS. If, during combustion of 1,3-butadiene, the same conditions (e.g., substrate flow rate) are maintained from run to run, then the soot properties remain constant. If, for example, flow rates are increased dramatically, the same products are formed, but at lower yields.

Results of electrochemical studies and those from ESR analysis of ascorbate radicals generated in a dose-dependent manner by BSDE confirmed the presence of pro-oxidant activity. This activity, however, was not related to the solid-state soot radical (Figure 4). This radical was unaltered by treatment with ascorbate and was unaffected by aging (18 months) of the soot. The stability and longevity of the solid-state radical and its presence in filtered, clarified BSDE suggests its possible utility as an environmental and biologic probe (i.e., of soot production and exposure). Conversely, POBN spin-trap results confirmed the presence of a very strong, reactive oxidant. This oxidant system was temporally dynamic, with radical products evolving and being trapped for > 24 hr. This time frame of oxidant evolution is on the same order as that of the toxicologic endpoints reported here. These data indicate that BSDE has strong oxidative properties that persist over biologically relevant time frames.

By virtue of their anatomic location, NHBE cells are putative targets *in vivo* for inhaled submicron particles that are present in urban and/or industrial particulate mixtures. Therefore, we selected NHBE cells as the targets for toxicologic studies with BSDE. Cytoplasmic fluorescence was the earliest and most striking response of the cells to BSDE exposure. Fluorescence was evident in the low-dose cells, very prominent in the high-dose group and absent from controls (Figure 6). These effects could be detected as early as 4 hr after exposure. There was no evidence of nuclear fluorescence up to 72 hr.

Cytoplasmic fluorescence has been attributed to accumulation of both aromatic hydrocarbons (*17*) and oxidized macromolecules, including age-associated fluorescent pigments, e.g., lipofuscin (*18*). However, the absence of cytoplasmic fluorescence in control NHBE cells suggests that their response to BSDE is distinct from the prominent, punctate fluorescence that has been described in mammalian cells and that has been ascribed to lysosomal lipofuscin accumulation (*19*). The cytoplasmic fluorescence does not appear to be caused by intrinsic fluorescence of a BSDE component. The fluorescence emission spectrum of a whole-cell lysate from BSDE-treated cells differed from

Table 1. Dose-dependent cytotoxicity of BSDE in NHBE cells.

Treatment group[a]	Mean no. of viable cells[b]	Percent viable cells[c]	Percent cytotoxicity[d]
Vehicle control	435 ± 13	87 ± 3	
Low dose	395 ± 10	79 ± 2	9.2
High dose	354 ± 2	71 ± 1	18.6

[a]See "Materials and Methods" for description of treatment groups. [b]See "Materials and Methods" for staining and scoring procedures. Values shown are the mean ± SD (n = 3). [c]Values are the mean ± SD. These were determined by dividing the mean number of viable cells by the total number of cells scored. [d]Values are relative to the control group.

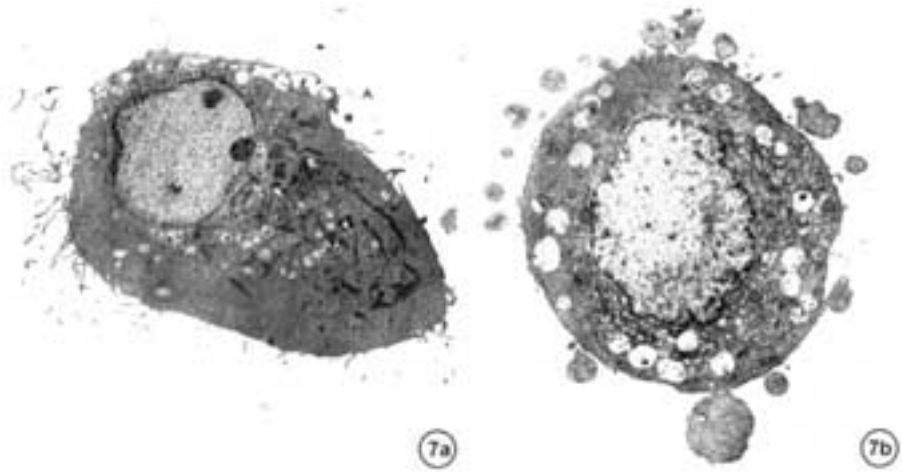

Figure 7. Low-magnification transmission electron micrographs of a vehicle-control (DMSO) NHBE cell (*A*) and a high-dose BSDE-exposed NHBE cell (*B*) 72 hr after a single acute exposure to BSDE. The cell surface in (*A*) is characterized by many microvillus-like surface projections. The cell surface in (*B*) is characterized by large blebs containing amorphous cytoplasmic material. The numerous microvilli seen in (*A*) are not apparent in (*B*). In (*B*) the cytoplasm is vesiculated and contains large peripheral vacuoles and swollen cisternae of the endoplasmic reticulum. Magnification = 2,500×.

Table 2. Dose-depependent induction of binucleated cells (BNCs) in NHBE cells after a single acute exposure to BSDE.

Treatment group[a]	Mean no. of BNCs[b]	Percent BNCs[c]
Vehicle control	20 ± 1	4.0 ± 0.2
Low dose	23 ± 1	4.6 ± 0.2
High dose	39 ± 4	7.8 ± 0.8

[a]See "Materials and Methods" for description of treatment groups. [b]Values shown are mean ± SD; these were determined by dividing the mean number of BNCs by the total number of cells scored. [c]Values are the mean percent BNCs by the total number of cells scored.

those of BSDE alone and of BSDE added to a lysate from vehicle-control NHBE cells (data not presented). It is more likely that NHBE fluorescence can be accounted for largely by protein denaturation, which begins early in cell death, continues even after cells have died, and is detected readily in unfixed tissue samples by ultraviolet microscopy. Fluorescence of altered (e.g., denatured, covalently modified) proteins as an early marker of cell death has been discussed in detail elsewhere (*20*).

Here, cellular fluorescence was detectable as early as 4 hr after treatment and varied with dose. Cell populations within treatment groups exhibited a range of fluorescence intensity, possibly corresponding to degrees of cell damage (Figure 6D,F). The presence in BSDE of a wide range of AHs and PAHs and of at least one strongly oxidizing component is consistent with these observations—the NHBE cell responses reflect acute oxidative damage.

Quantitation of the cell damage indicated by the fluorescence results was provided by the dye exclusion and BNC assays. Dose-dependent cytotoxicity was demonstrated in both strains of NHBE cells, 72 hr after exposure to BSDE. Although wide differences (1,000-fold) have been reported in the survival of different NHBE strains treated with chemical carcinogens (*21*,*22*), here both strains responded very similarly to the single BSDE challenge. The BSDE was only mildly cytotoxic, (~ 20% in the high-dose group) as estimated by Trypan Blue exclusion. This suggests that more subtle forms of damage than large-scale denaturation of proteins (e.g., genetic damage) might be produced *in vivo* and retained in otherwise viable BSDE-exposed cells, as the BNC results indicate.

BNCs appear spontaneously both *in vivo* and *in vitro* (*23*). They can result from an arrest in the G_2 phase of the cell cycle (*24*) and can be induced by chemicals (*14*,*25*) and radiation (*26*). BSDE elicited a dose-dependent increase in BNCs in NHBE cells (Table 2) similar to that observed in the phenotypically altered progeny of NHBE cells exposed to fractionated doses of α-particles (*26*). In addition, BNC formation has been proposed to be a form of genomic instability leading to altered DNA content in tumor cells (*27*). These independent studies (*26*,*27*) combined with the presence of known genotoxic agents in the BSDE lead us to postulate that the BNC formation observed here likely is a genotoxic response.

A fraction of BSDE-treated cells exhibited major morphologic alterations, including swelling both of the cytoplasm and endoplasmic reticulum, cytoplasmic vacuolization, and extensive plasma membrane blebbing. These changes are characteristic of oncosis, an ischemia-induced process of accidental cell death (*20*,*28*,*29*).

The chemical analyses here reveal the presence of known carcinogens/mutagens in high amounts and of highly reactive oxidizing species. The combination of these findings with the moderate cytotoxicity and genotoxicity in NHBE cells exposed to BSDE is provocative. BSDE, or a similar complex mixture, would be expected to be procarcinogenic by virtue of its interference with normal cell division combined with its relatively mild cytotoxicity to target cells along the respiratory tract (i.e., NHBE cells). Thus, *in vivo* investigations of the potential carcinogenicity, as well as of other respiratory and cardiovascular effects, of BSDE and similar complex mixtures are warranted.

References and Notes

1. Louisiana Office of Public Health. 1999 Louisiana Health Report Card, Vol. 38. New Orleans, LA:Louisiana Office of Public Health, 1999.
2. Kodavanti UP, Costa DL, Bromberg PA. Rodent models of cardiopulmonary disease: their potential applicability in studies of air pollutant susceptibility. Environ Health Perspec 106(suppl 1):111–130 (1998).
3. Bayram H, Devalia J, Sapsford R, Ohtoshi T, Miyabara Y, Sagai M, Davies R. The effect of diesel exhaust particles on cell function and release of inflammatory mediators from human bronchial epithelial cells *in vitro*. Am J Respir Cell Mol Biol 18:441–448 (1998).
4. Boland S, Baeza-Squiban A, Fornier T, Houcine O, Gendron M, Jouvenot G, Coste A, Aubier M, Marano F. Diesel exhaust particles are taken up by human airway epithelial cells *in vitro* and alter cytokine production. Am J Physiol 276:L604–613 (1999).
5. Boland S, Bonvallot V, Fournier T, Baeza-Squiban A, Aubier M, Marano F. Mechanisms of GM-CSF increase by diesel exhaust particles in human airway epithelial cells. Am J Physiol Lung Cell Mol Physiol 278:L25–32 (2000).
6. Hashimoto S, Gon Y, Takeshita I, Matsumoto K, Jibiki I, Takizawa H, Kudoh S, Horie T. Diesel exhaust particles activate p38 MAP kinase to produce interleukin-8 and RANTES by human bronchial epithelial cells and *N*-acetylcysteine attenuates p38 MAP kinase activation. Am J Respir Crit Care Med 161:280–285 (2000).
7. Carter J, Ghio A, Samet J, Devlin R. Cytokine production by human airway epithelial cells after exposure to an air pollution particle is metal-dependent. Toxicol Appl Pharmacol 146:180–188 (1997).
8. Quay J, Reed W, Samet J, Devlin R. Air pollution particles induce IL-6 gene expression in human airway epithelial cells via NF-kB activation. Am J Respir Cell Mol Biol 19:98–106 (1998).
9. U.S. Environmental Protection Agency. National ambient air quality standards for particulate matter: final rule. Fed Reg 62:138 (1997).
10. Pollution Locator-Criteria Air Pollutants in 1998, Rank Counties by Health Risks. Environmental Defense Fund: In Your Community. Available: http://www.scorecard.org/scorecard/index) [cited 11 January 2001].
11. Info Louisiana: LA Maps & Geographical Information. Available: http://www.state.la.us/state/map.htm [cited 11 January 2001].
12. Catallo WJ. Polycyclic aromatic hydrocarbons in combustion residues from 1,3-butadiene. Chemosphere 16:1053–1063 (1998).
13. Pou S, Ramos C, Gladwell T, Renks E, Centra M, Young D, Cohen M, Rosen G. A kinetic approach to the selection of a sensitive spin trapping system for the detection of hydroxyl radical. Anal Biochem 217:76–83 (1994).
14. Rodilla V, Pellicer JA, Pertusa J, Mothersill C. Induction of micronucleated and binucleate cells in Chinese hamster ovary (CHO) cells by *cis*-diaminedichloroplatinum (II): a morphological and morphometric study. Mutat Res 241:115–124 (1990).
15. Allen J, Durant J, Dookeran N, Taghizadeh K, Plummer E, Lafleur A, Sarofim A, Smith K. Measurement of $C_{24}H_{14}$ polycyclic aromatic hydrocarbons associated with a size-segregated urban aerosol. Environ Sci Technol 32:1928–1932 (1998).
16. Waterman D, Horsfield B, Leistner F, Hall K, Smith S. Quantification of polycyclic aromatic hydrocarbons in the NIST standard reference material (SRM1649A) urban dust using thermal desorption GC/MS. Anal Chem 72:3563–3567 (2000).
17. Roque A, Ackren J. Enzymatic changes in fluorescent alveolar macrophages of the lungs of cigarette smokers. Acta Cytol 12:420–429 (1968).
18. Ames B, Shigenaga M, Hagan T. Oxidants, antioxidants and the degenerative diseases of aging. Proc Natl Acad Sci USA 90:7915–7922 (1993).
19. Andersson H, Baechi T, Hoechl M, Richter C. Autofluorescence of living cells. J Microsc 191:1–7 (1998).
20. Majno G, Joris I. Cells. Tissues and Disease: Principles of General Pathology. Boston:Blackwell Science, Inc., 1996.
21. Sigfried J, Nesnow S. Cytotoxicity of chemical carcinogens towards human bronchial epithelial cells evaluated in a clonal assay. Carcinogenesis 5:1317–1322 (1984).
22. Sigfried J, Rudo K, Bryant B, Ellis S, Mass M, Nesnow S. Metabolism of benzo(*a*)pyrene in monolayer cultures of human bronchial epithelial cells from a series of donors. Cancer Res 46:4368–4371 (1986).
23. Beams H, King R. The origin of binucleate and large mononucleate cells in the liver of the rat. Anat Rec 83:281–297 (1942).
24. Ronot X, Hecquet C, Larno B, Hainque B, Adolphe M. G_2 arrest, binucleation and single-parameter DNA flow cytometric analysis. Cytometry 7:286–290 (1986).
25. Pellicer J, Pertusa J, Alcober V. Binucleate cells in the Ehrlich ascites tumor. Action of 5-fluorouracil. Biol Cell 60:255–258 (1987).
26. Kennedy C, Mitchell C, Fukushima N, Neft R, Lechner J. Induction of genomic instability in normal human bronchial epithelial cells by ^{238}Pu alpha particles. Carcinogenesis 17:1671–1676 (1996).
27. Fukosawa K, Vande Woude G. *Mos* overexpression in Swiss 3T3 cells induces meiotic-like alterations of the mitotic spindle. Proc Natl Acad Sci USA 92:3430–3434 (1995).
28. Majno G, Joris I. Apoptosis, oncosis and necrosis. Am J Pathol 146:3–15 (1995).
29. Penn A, Henk W, Kennedy CH, Catallo WJ. Unpublished data.